THE JOURNAL OF BIOLOGICAL CHEMISTRY VOL. 286, NO. 33, pp. 29366–29375, August 19, 2011

A Conserved Non-canonical Motif in the Pseudoactive Site of the ROP5 Pseudokinase Domain Mediates Its Effect on Toxoplasma Virulence*[S]

Received for publication, April 20, 2011, and in revised form, June 21, 2011 Published, JBC Papers in Press, June 27, 2011, DOI 10.1074/jbc.M111.253435

Michael L. Reese[1] **and John C. Boothroyd**[2]

From the Department of Microbiology and Immunology, Stanford University School of Medicine, Stanford, California 94305-5124

The ROP5 family is a closely related set of polymorphic pseudokinases that are critical to the ability of *Toxoplasma* to cause disease. Polymorphisms in ROP5 also make it a major determinant of strain-specific differences in virulence. ROP5 possesses all of the major kinase motifs required for catalysis except for a substitution at the catalytic Asp. We show that this substitution in the catalytic loop of ROP5 is part of a motif conserved in other pseudokinases of both *Toxoplasma* and human origin, and that this motif is required for the full activity *in vivo* of ROP5. This suggests evolutionary selection at this site for a biochemical function, rather than simple drift away from catalysis. We present the crystal structures of a virulent isoform of ROP5 both in its ATP-bound and -unbound states and have demonstrated that despite maintaining the canonical ATP-binding motifs, ROP5 binds ATP in a distorted conformation mediated by unusual magnesium coordination sites that would not be predicted from the primary sequence. In addition, we have mapped the polymorphisms spread throughout the primary sequence of ROP5 to two major surfaces, including the activation segment of ROP5. This suggests that the pseudoactive site of this class of pseudokinases may have evolved to use the canonical ATP-binding motifs for non-catalytic signaling through allostery.

Proteins involved in cellular signaling often have modular domain structure; whereas enzymatic domains catalyze the reactions that propagate a signal, the precise subcellular localization of a protein, and the recognition of partner molecules are usually accomplished by nonenzymatic domains (1, 2). Complicating this paradigm, noncatalytic enzymatic domains such as pseudokinases have been recognized as important regulators of signaling networks, for example, by acting as molecular scaffolds for an effector and its downstream targets, or by modulating the activity of a catalytically active enzyme (3).

The cellular signaling occurring at the interface between an intracellular pathogen and its host cell is particularly complex. *Toxoplasma gondii* is an obligate, intracellular parasite with the unusual ability to infect almost any nucleated cell of virtually any warm-blooded animal. During infection, *Toxoplasma* secretes a variety of effector molecules into its host cell to monitor and co-opt host signaling networks (4, 5). Although these effectors originate in the specialized secretory organelles of the parasite, called rhoptries (and thus the designation of these effectors as "ROPs"), they carry out their various functions in the cytosol of the host cell. Three ROPs have been identified as active kinases that drastically alter host signaling (6, 7) and disease outcome (6, 8, 9). Indeed, of the ~160 predicted kinases of *Toxoplasma*, at least one-third are predicted to be secreted into the host cell (7), suggesting an active role in pathogenesis.

Intriguingly, the kinome of the *Toxoplasma*, especially its secreted effectors, is highly enriched in pseudokinases. We and others previously identified a closely related family of these secreted pseudokinases, the ROP5 family, as absolutely critical to pathogenesis in mice; ablation of the locus results in a complete loss of virulence in mice (10, 11). The ROP5 family is encoded by a locus of tandemly duplicated genes that are highly polymorphic (supplemental Fig. S1). Allelic variation of these isoforms is concentrated within the pseudokinase domains and is responsible for a $>10^5$ difference in virulence (LD_{50}) in a mouse model of disease (10).

There is an abundance of structural information on active protein kinases, which has led to a detailed understanding both of the reaction mechanism of phosphoryl transfer and various methods of regulation by diverse actors such as small molecules (12) and both *cis*- (13) and *trans*- acting protein-protein interactions (14). Pseudokinases, however, remain something of a functional mystery. Recent structures of the pseudokinase domains of HER3 (15), ILK (16), and STRADα (17) have suggested these proteins act as "smart" scaffolds that allosterically regulate their binding partners. Other studies have indicated that some proteins originally predicted to be pseudokinases may catalyze phosphoryl transfer through atypical means (18–20).

Most studies of pseudokinases to date have concentrated on those residues that are missing from the canonical kinase motifs. The ROP5 family is a closely related family of proteins (up to 10 paralogous ROP5 genes exist within a given strain) under extraordinary selective pressure, and thus provides an opportunity to examine the functional relevance of conserved substitutions within the canonical kinase motifs (*i.e.* things conserved in pseudokinases that are divergent from an active kinase). Here, we present such an examination, guided by the crystal structure of the ROP5 pseudokinase domain, and demonstrate the *in vivo* relevance of a key substitution in the pseu-

* This work was supported, in whole or in part, by National Institutes of Health Grant AI73756.

[S] The on-line version of this article (available at http://www.jbc.org) contains supplemental Figs. S1–S9.

[1] Supported, in part, by a postdoctoral fellowship from the American Cancer Society.

[2] To whom correspondence should be addressed: Fairchild Building, Rm. D305, 299 Campus Dr., Stanford, CA 94305-5124. Tel.: 650-723-7984; Fax: 650-725-6757; E-mail: john.boothroyd@stanford.edu.

doactive site to function for ROP5 in determining the outcome of *Toxoplasma* infection.

EXPERIMENTAL PROCEDURES

Parasite Culture and Genetic Manipulation—Human foreskin fibroblasts were grown in Dulbecco's modified Eagle's medium supplemented with 10% fetal bovine serum and 2 mM glutamine. *Toxoplasma* tachyzoites were maintained in confluent monolayers of human foreskin fibroblasts. Complemented RHΔ*rop5* strains were created by electroporating 15 μg of linearized plasmid for the targeted replacement of the *UPRT* locus (21) with the *ROP5* wild-type or mutant of choice. Clonal parasites were grown from populations by limiting dilution.

Cloning and Plasmid Construction—DNA encoding residues 171–540 of $ROP5B_I$ was amplified by PCR using Phusion polymerase (New England Biolabs) from a plasmid encoding the *Toxoplasma* genomic locus for its gene, and cloned into the pET28a (Novagen) bacterial expression vector between the NdeI and XhoI sites. Mutagenesis was carried out according to the Phusion protocol. DNA encoding the R389D mutant $ROP5A_{III}$ gene, including its native promoter (~600 bp upstream from start) was cloned into a previously described vector (10) in-frame with a C-terminal HA tag and the *Toxoplasma* GRA2 3′-UTR, flanked by sequences for targeted recombination into the *Toxoplasma* uracil-phosphoribotransferase locus.

Immunofluorescence and Western Blot—For immunofluorescent analysis, cells were permeabilized and blocked for 1 h in PBS, 0.1% Triton X-100, 3% BSA. Cells were incubated for 2 h at room temperature with mouse monoclonal antibodies ROP2/4 (mAb T34A7, gift of J.-F. Dubremetz) or rat anti-HA (3F10, Roche Applied Science) at 1:200 and 1:500 dilution, respectively, in PBS, 3% BSA. Cells were washed 3 times with PBS and incubated for 1 h with anti-rat Alexa 488- and anti-mouse Alexa 594-conjugated secondary antibodies (Molecular Probes). Cells were again washed 3 times with PBS and mounted in VectaShield (Vector). Wide-field images were captured at ×100 on an Olympus BX60 and a Hamamatsu Orca100 CCD. For Western blot analysis, samples were separated by SDS-PAGE, transferred to a PVDF membrane (Millipore), and blocked in Tris-buffered saline, pH 7.5, with 0.01% Tween with 5% milk powder for 1 h. Membranes were then incubated for 2 h with HRP-conjugated rat anti-HA at a dilution of 1:500 in blocking buffer. Membranes were washed 3 times with TBST, and visualized with ECL reagent (Pierce). The membranes were then stripped, reblocked, and probed with primary mouse anti-SAG1 at 1:20,000 dilution for 2 h. After washing, membranes were probed for 1 h with HRP-conjugated secondary, washed again, and visualized as above.

Mouse Survival Analysis—10–12-Week-old female BALB/c (Jackson Labs) mice were infected by peritoneal injection with parasites diluted to the appropriate dose in phosphate-buffered saline, pH 7.4, and monitored daily for survival. Dosage was verified by plaque assay of inoculum. Infection of surviving mice was verified by testing serum for reactivity with *Toxoplasma* lysate. Data were analyzed in Prism (GraphPad Software) using the log-rank survival test.

Protein Expression and Purification—All recombinant protein was expressed in *Escherichia coli* Rosetta2(DE3) (EMD Biosciences). $ROP5B_I$ was purified on nickel-nitrilotriacetic acid resin (Qiagen), the His_6 tag was removed by overnight thrombin cleavage at 4 °C and further purified by anion exchange and gel filtration chromatography. His_6-ROP16-HA was purified as previously described (22).

ATP-binding Experiments—Purified recombinant protein was incubated at 4 °C with a 30-μl bed volume of γ-linked ATP-Sepharose (Innova Biosciences) in 10 mM Tris, pH 8.0, 150 mM NaCl, 2 mM DTT, 10 mM $MgCl_2$, 0.1% Triton X-100. The beads were sedimented and briefly washed with 1 ml of buffer before protein was eluted in SDS loading buffer. Binding was analyzed by SDS-PAGE stained with Coomassie Blue.

Crystallization—The crystals of $ROP5B_I$ (apo form) were grown at 18 °C by mixing equal volumes of protein solution (~0.5 mM; 10 mM HEPES, pH 7.0, 100 mM NaCl) and a reservoir containing 20% polyethylene glycol 3350, 10 mM $MgCl_2$, and 0.3 M sodium malonate, pH 5.0. The ATP bound crystals were grown in a similar condition with the addition of 10 mM ATP and 20 mM $MgCl_2$. To generate a platinum derivative, $ROP5B_I$ (apo) crystals were soaked with 10 mM K_2PtCl_4 for 2 h, washed quickly in mother liquor, and frozen. All crystals were flash frozen in a cryoprotectant of mother liquor with 30% ethylene glycol.

Data Collection, Structure Determination, and Refinement—The diffraction data for native crystals were collected at beamline 11.1 of SSRL (the Stanford Synchrotron Radiation Laboratory) at a wavelength of 1.00 Å and a temperature of 100 K. Data for the apo-$ROP5B_I$ platinum derivatives were collected in an inverse beam experiment at a wavelength of 0.979 Å. Integration, indexing, and scaling of the diffraction data were performed using the HKL2000 suite of programs (23). Initial phases at 2.7 Å were determined by single isomorphous replacement with anomalous scattering from two well occupied platinum sites and used to generate a starting model after density modification with the SOLVE/RESOLVE package (24, 25). The high resolution native data were incorporated for extension and map improvement in Phenix (26). Manual rebuilding in Coot (27) and refinement in Phenix led to a final 1.90-Å structure of apo-$ROP5B_I$, which was deposited in the Protein Data Bank (PDB)[3] (PDB accession 3Q5Z). Phases for the ATP-bound $ROP5B_I$ structure were determined by molecular replacement using Phaser (28) with apo-$ROP5B_I$ as a search model. Good density was observed for the bound ATP, two Mg^{2+} ions, and coordinating waters. The model was built and refined using Coot and Phenix, with a final resolution of 1.72 Å (PDB accession 3Q60). Both the apo- and ATP-bound models have excellent stereochemistry with no residues in disallowed regions (96.9 and 96.2% favored for the apo- and ATP-bound, respectively) from Ramachandran plots as validated by the program MOLPROBITY (29).

In Vitro Kinase Activity Assay—Either 10 ng of recombinant ROP16 or up to 10 μg of wild-type or H389D $ROP5B_I$ was incubated with 1 μg of substrate (either histone H1 or dephos-

[3] The abbreviations used are: PDB, Protein Data Bank; NTE, N-terminal extension.

TABLE 1

Human and *Toxoplasma* kinases in which the Arg preceding the catalytic base has been substituted for a Gly

HRD motif and predicted activities are noted. HGB pseudokinases are boxed. *Toxoplasma* proteins predicted to be secreted into the host cell are starred.

Human			*Toxoplasma*		
Kinase	Predicted Active	HRD	Kinase	Predicted Active	HRD
Bub1, BubR1, Bud32, NIK, VRK1, VRK2, IRAK1, TOPK	Yes	HGD	ROP16*, ROP17* ROP31*, ROP32* ROP46*, TGME49_083790, TGME49_021550	Yes	HGD
STYK1	No	HGD	ROP24*	No	HGD
Trbl1	No	LGD	ROP37*	No	HGN
VRK3, ANPa, JAK1, JAK2, JAK3, TYK2, SCYL2, NRBP1, NRBP2	No	HGN	TGME49_036620	No	HGS
ANPb, SgK396	No	HGS	ROP5A$_I$*, TGME49_050680 (putative TBCK)	No	HGR
IRAK3	No	CGS	ROP4*, ROP7*, ROP42*, ROP43*, ROP44*	No	HGK
CygD, CygF Hser	No	HGR	ROP5B$_I$*, ROP5C$_I$* ROP36*	No	HGH
MLKL	No	HGK	TGME49_120000 (putative SCYL)	No	HGL
Slob	No	YGH			

phorylated myelin basic protein) in a 50-μl volume using protein kinase buffer (New England Biolabs) with 20 μCi of [γ-^{32}P]ATP (PerkinElmer Life Sciences) for 1 h at 37 °C and halted by addition of SDS-loading buffer and boiling. The completed reactions were separated by SDS-PAGE, the gel was dried and exposed overnight to a phosphorscreen (GE Healthcare).

RESULTS

A Conserved Pseudokinase Pseudoactive Site Motif Is Required for Efficient ROP5 Function—As previously reported, polymorphisms between the various allelic isoforms of ROP5 are concentrated in the predicted pseudokinase domain (supplemental Fig. S1), which appears to be under strong, positive selection (10). It is striking, however, how well the residues comprising the former active site are conserved within the family, strongly suggesting a functional significance: save for the catalytic Asp (the D of the well studied "HRD" motif of active kinases), ROP5 possesses the canonical residues at each of the major positions required for ATP binding and catalysis. In ROP5, the catalytic Asp in the HRD motif is replaced with either an Arg or His depending on the ROP5 isoform. It is intriguing that these substitutions both replace the acidic Asp with a basic residue.

To determine how common such a substitution is in other pseudokinases, we examined the predicted sequences of the complete human and *Toxoplasma* kinomes. It is important to note that although *Toxoplasma* is genetically distant from mammals, many of its kinases are secreted into the cytosol of its mammalian hosts, where they exert their end function. As ~30% of the predicted active kinases and pseudokinases of *Toxoplasma* are from a single family of homologous proteins specific to coccidian parasites (the so-called "rhoptry kinases" (7), which includes ROP5), similarities between these kinases and mammalian kinases are likely due to true convergent evolution rather than other mechanisms, such as horizontal gene transfer.

The Arg of the ROP5 HRD has been replaced with a Gly in each of the isoforms (Table 1 and supplemental Fig. S1). Although such a substitution would not, itself, be predicted to interfere with catalytic activity, it is, however, a remarkably rare substitution among human kinases and is highly predictive of a pseudokinase: only 27 of the ~500 human proteins with kinase folds possess it, and of these, 19 are predicted pseudokinases (representing ~40% of human pseudokinases; Table 1). The remaining 8 active kinases are enriched in proteins that are closely related to known pseudokinases (*e.g.* VRK2, IRAK1). Of these human "Gly" pseudokinases, very few residues appear as replacements for the catalytic Asp (Table 1), which can be clustered into two classes: short polar (Ser/Asn) and basic (His/Arg/Lys). Interestingly, this appears to be the case in *Toxoplasma* pseudokinases, as well (Table 1). Furthermore, the correlation is symmetric: of the 16 *Toxoplasma* and human pseudokinases with a basic residue substituted for the catalytic Asp, all but one are preceded by a Gly (Fig. 1*A*). It is important to note that even within the kinome of the organism, many of these pseudokinases appear to have evolved independently from one another; in both the human and *Toxoplasma* examples many of the members are more closely related to another, often active, kinase than to one another (Fig. 1*A*). Thus, such substitutions appear to identify a distinct subclass of pseudokinase, in which the HRD motif is replaced with an HGB tripeptide (where "B" denotes a basic residue).

We next set out to determine whether this conserved but noncanonical motif in the ROP5 pseudoactive site was contributing to the function of ROP5. We had previously created a strain in which the entire ROP5 locus had been deleted (Δ*rop5*), which resulted in the complete attenuation of an otherwise highly virulent strain (10). We also demonstrated that a single copy of the ROP5A$_{III}$ isoform was able to partially complement the virulence phenotype. This provided the ideal background to address our current question. We reasoned that a charge swap returning the ROP5 HGB motif to an HGD was the most likely to affect ROP5 function without causing structural problems. Thus, we created a parasite line in which the only ROP5 expressed was ROP5A$_{III}$ R389D. The gene was targeted to the identical locus as the wild-type copy, creating an isogenic par-

A

Gene	Closest Relative	Gly-rich P-loop	VAI**K**	HR**D**	**D**FG
T. gondii					
ROP5A$_I$		No	FAL**K**	HG**R**	**D**VS
ROP5B$_I$	ROP18	No	FAL**K**	HG**H**	**D**VS
ROP5C$_I$		No	FAL**K**	HG**H**	**D**VS
ROP4	ROP2, ROP8	No	RNE**G**	HG**K**	**D**FG
ROP7		No	RHQ**A**	HG**K**	**D**FG
ROP22	ROP36	No	Cryptic	HT**H**	**D**LN
ROP36	ROP22	No	FVV**K**	HG**H**	**D**FH
ROP42		Yes	LAV**K**	HG**K**	**D**LG
ROP43	ROP17, ROP31	Yes	LAV**K**	HG**K**	**D**LG
ROP44		Yes	LAV**K**	HG**K**	**D**LG
TBCK	TGME49_036620	No	Cryptic	HG**R**	**D**WG
H. sapiens					
Hser	ANPa	No	VIL**K**	HG**R**	**D**FG
CygD	CygF	No	VWL**K**	HG**R**	**D**HG
CygF	CygD	No	VWL**K**	HG**R**	**D**YG
MLKL	MLK1	No	VAI**K**	HG**K**	**G**FE
Slob	SgK307, SgK424	No	Cryptic	YG**H**	Cryptic

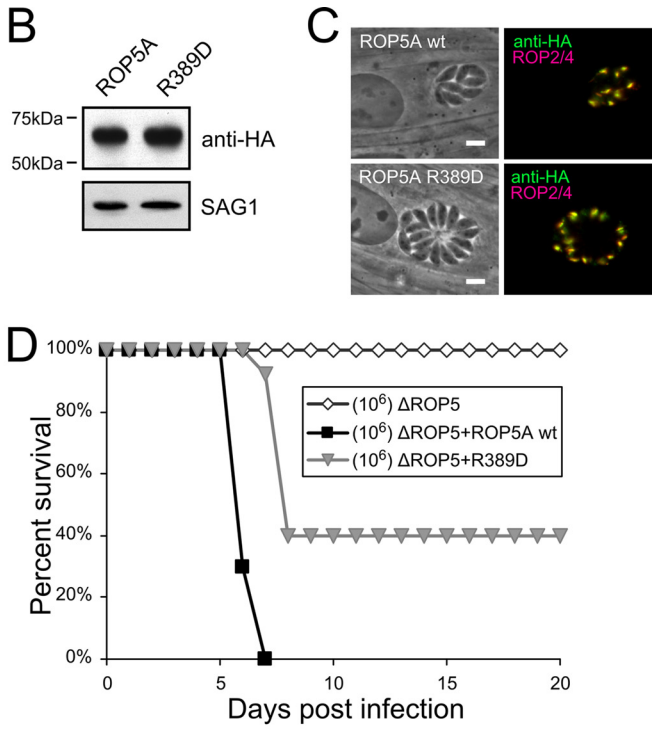

FIGURE 1. **The noncanonical ROP5B$_I$ HRD motif contributes to its function *in vivo*.** *A*, table of HGB pseudokinases, where *B* indicates a basic residue (His/Lys/Arg). Substitutions at other motifs are indicated, as is the closest relative of each pseudokinase, which are based on previously published alignments (7, 48). *B,* Western blot of lysates from Δ*rop5* parasites transgenic for ROP5A$_{III}$-HA or ROP5A$_{III}$(R389D)-HA. The blot was probed with antibodies recognizing the HA tag and the parasite SAG1 protein as a loading control. *C,* localization of the HA-tagged ROP5 proteins (*green*) in the parasites described above was compared with the rhoptry marker ROP2/4 (*red*). *Scale bar* is 5 μm. *D,* BALB/c mice were injected intraperitoneally with 10^6 parasites of either Δ*rop5* or Δ*rop5* complemented with either wild-type ROP5A$_{III}$-HA or ROP5A$_{III}$(R389D)-HA and monitored for mortality. $n = 5$ mice for Δ*rop5*; $n = 25$ mice for complemented strains.

asite strain, except for the single point mutation. Both the wild-type and R389D ROP5A were expressed in-frame with a C-terminal HA tag, allowing us to validate the localization to the parasite rhoptries and equivalent protein expression of ROP5 in both strains (Fig. 1, *B* and *C*).

Mice were then challenged with equal doses of either the Δ*rop5*, or the strains complemented with either wild-type or R389D ROP5A$_{III}$ (Fig. 1*D*). Interestingly, the mutant ROP5 protein maintained its ability to at least partially complement the virulence phenotype. However, whereas infection with parasites expressing wild-type ROP5A$_{III}$ was uniformly lethal to mice, a portion of the mice infected with the R389D strain survived. In addition, the median survival time of the mice who succumbed to infection was significantly shifted ($p < 0.0001$ by log-rank analysis), strongly indicating that the mutant protein was not as efficient in mediating its effect on virulence as the wild-type protein.

These data are particularly intriguing in the context of the large amount of mutation data for a variety of active kinases. A partial attenuation of activity is contrary to what one would expect from the similar mutation of an active kinase; such mutations ablate the normal function of kinase, and are usually completely unable to complement a phenotype. In fact, mutation of the active site of the kinase often creates a dominant-negative phenotype that can disable the wild-type kinase in the same cell. Given that the mutation appears to not disrupt the stability or trafficking of the protein, our data suggest that the pseudoactive site of ROP5 is involved in its function, but is indeed not catalytic. It is, however, possible that the R389D mutation "rescued" ROP5 kinase activity, and it was this unintended kinase activity that was reducing the effect of ROP5 on virulence *in vivo*.

To rule this out, we created an additional *Toxoplasma* strain, in which the only ROP5 expressed was ROP5A$_{III}$ carrying both R389D and K263S mutations. This latter mutation alters the Lys of the VAIK motif, which makes contacts with the β-phosphate of ATP and is required for catalysis in active kinases (30). It should be noted that among the human and *Toxoplasma* HGB pseudokinases, 11 of 16 have conserved the VAIK Lys, and 14 of 16 have conserved the DFG Asp, suggesting that these pseudokinases have conserved the ability to bind ATP. Although a portion of the ROP5A R389D/K263S mutant was correctly localized to the rhoptries, some of the protein appeared to be trapped in the endoplasmic reticulum or Golgi of the parasites (supplemental Fig. S2). This is consistent with protein that is either misfolded or is unable to make an interaction that is critical for its trafficking to the rhoptries. Not surprisingly, such mutant ROP5 was unable to complement the virulence of the ΔROP5 parasites (supplemental Fig. S2). We also observed either similar mislocalization or undetectable expression of ROP5 in multiple independent transfections to express protein with the single mutation K263S. This suggests

that wild-type ROP5 binds ATP, and that this interaction with nucleotide promotes the maturation and trafficking of the protein. This interpretation is consistent with the behavior of active kinases, such as PKC, in which similar mutations that reduce the affinity of the protein for ATP disrupt the correct maturation of the protein (31). Due to the partial mislocalization of the ROP5 protein, these mutants were, however, otherwise uninformative as to the function of ROP5. We thus felt it necessary to move to *in vitro* studies of the biochemistry of ROP5.

ROP5 Binds ATP But Is Catalytically Inactive—To gain further insight into the function of ROP5 we sought to directly test whether wild-type or mutant protein had catalytic activity. Although we had difficulty obtaining suitable quantities of the pseudokinase domain of $ROP5A_{III}$, we were able to recombinantly express and purify $ROP5B_I$, which we used in all of our *in vitro* assays. Although there are many residues that are polymorphic between the virulent alleles of the ROP5A and ROP5B isoforms (supplemental Fig. S1), the residues of the pseudoactive site are well conserved (aside from the catalytic base), suggesting that the biochemical properties of the individual purified proteins should be similar. As discussed above, ROP5 lacks the kinase catalytic base (the "HRD" Asp has been replaced by Arg-389 or His-389, depending on isoform; supplemental Fig. S1), resulting in its predicted catalytic inactivity. However, ROP5 has conserved residues that are known to coordinate both Mg^{2+} and ATP in active kinases (Asp-407 and Asn-394 in ROP5; supplemental Fig. S3). To test whether ROP5 was competent to bind ATP, we incubated recombinantly expressed and purified $ROP5B_I$ with γ-phosphate-linked ATP-Sepharose, washed the resin, eluted the bound protein with SDS-loading buffer and EDTA, and evaluated the binding by SDS-PAGE. As expected, ROP5 was efficiently pulled-down by the ATP resin in a Mg^{2+}-dependent manner and excess soluble ATP competitively inhibited this interaction (Fig. 2*A*).

We tested the same recombinant protein for *in vitro* kinase activity. We incubated purified, recombinantly expressed $ROP5B_I$ with two standard substrates and [γ-^{32}P]ATP and measured the level of phosphorylation by autoradiogram (Fig. 2*B*). Although ~0.01 μg of recombinantly expressed ROP16, a paralog that we have previously demonstrated to be an active kinase (22), was efficiently autophosphorylated, even 10 μg of ROP5 produced no detectable autophosphorylation nor phosphorylation of myelin basic protein or histone H1. This is consistent with current understanding of the protein kinase reaction mechanism, in which the invariant catalytic Asp is thought to accept the proton from the substrate hydroxyl (32, 33).

As ROP5 appears to differ from active kinases only in that it lacks the catalytic Asp, we reasoned that by mutating His-389 of $ROP5B_I$ to Asp, we might "rescue" the kinase activity of ROP5. $ROP5B_I$ H389D expressed well and was similarly soluble to the wild-type protein. As expected, the mutant protein maintained its ability to bind ATP (Fig. 2*A*). Importantly, however, we were unable to detect *in vitro* kinase activity from $ROP5B_I$ H389D (Fig. 2*B*), suggesting that the conformation of the ATP-bound ROP5 active site was somehow distorted from that required for phosphoryl transfer. These data also strongly suggest the difference in virulence we observed *in vivo* with our $ROP5A_{III}$ R389D mutant was not due to aberrant kinase activity.

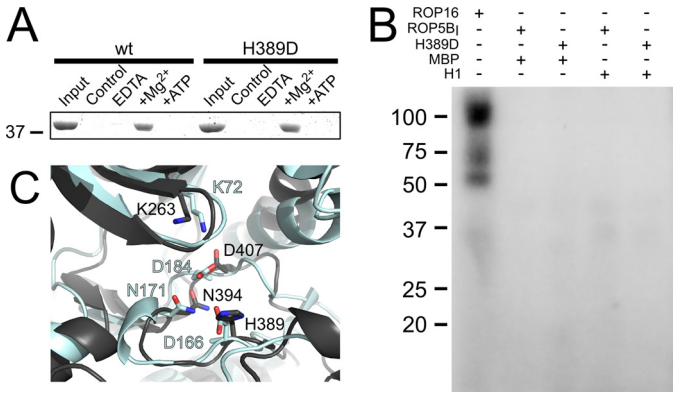

FIGURE 2. **ROP5 can bind ATP, but is catalytically inactive.** *A*, $ROP5B_I$ was incubated with γ-linked ATP-Sepharose in the presence of EDTA, $MgCl_2$, or $MgCl_2$ and 1 mM ATP. Protein was separated by SDS-PAGE and visualized with Coomassie Blue. *Control* indicates Sepharose without cross-linked ATP in the presence of $MgCl_2$. *B*, representative *in vitro* radioactive kinase assay data using bacterially expressed, purified recombinant protein. Either 10 ng of the catalytically active *Toxoplasma* kinase ROP16 or 10 μg of wild-type or mutant $ROP5B_I$ (H389D) were incubated with substrate in the presence of [γ-^{32}P]ATP. Substrates used were recombinant histone H1 (*H1*) or myelin basic protein (*MBP*). The multiple bands in the ROP16 lane likely correspond to multiple autophosphorylated species. *C*, the active sites of ATP-unbound $ROP5B_I$ (*black*) is overlaid on that of the ATP-bound structure of PKA (*light blue*, PDB code 1ATP). Residues important for ATP binding and catalysis in PKA are represented as *sticks* and numbered according to their position in $ROP5B_I$ and PKA, respectively. The PKA ATP and alternate conformation of $ROP5B_I$ His-389 are not shown for clarity.

To gain insight into the structural basis for the lack of activity of ROP5, we solved the crystal structure of the apo-$ROP5B_I$ pseudokinase domain using the single isomorphous replacement with anomalous scattering method with native data to 1.9 Å and a platinum derivative with data to 2.1 Å. The final model was completed using native data to 1.9 Å (crystallographic information in Table 2). We then compared our crystal structure of ROP5 to that of PKA. Save for its missing catalytic Asp, the active site of ROP5 appears structurally similar to an active kinase; all of the major motifs involved in ATP binding overlaid with those of ATP-bound PKA (Fig. 2*C*), suggesting ROP5 should bind ATP in a similar mode.

ROP5 Uses Canonical Residues to Bind ATP in a Conformation Unsuitable for Catalysis—We next sought to determine the structure of the ATP-bound conformation of ROP5. Crystals of $ROP5B_I$ were grown in the presence of ATP and $MgCl_2$ and a native dataset were collected to 1.72 Å. The structure was solved by molecular replacement using the apo-$ROP5B_I$ structure as a search model. Consistent with the lack of catalytic activity of ROP5, the nucleotide was completely unhydrolyzed during crystallization. Strong electron density was found for all atoms of ATP, its two coordinated Mg^{2+} cations, and their associated water molecules. Surprisingly, the structure of $ROP5B_I$ was unchanged upon binding ATP; the two structures have a root mean square deviation of 0.8 Å for 313 of 351 Cα atoms, and neither the P-loop nor the activation segment show significant movement in the two structures (Fig. 3*A* and supplemental Fig. S4) This is consistent with the recently solved structures of other pseudokinases that lack a Gly-rich P-loop:

TABLE 2
Data collection and refinement statistics

Data collection	Apo-ROP5B$_I$ (platinum)	Apo-ROP5B$_I$ native	ROP5B$_I$:ATP
Space group	$P2_12_12$	$P2_12_12$	$P2_12_12$
Cell dimensions			
a, *b*, *c* (Å)	116.98, 69.83, 43.30	117.34, 70.55, 43.01	123.36, 69.33, 43.39
α, β, γ (°)	90, 90, 90	90, 90, 90	90, 90, 90
Resolution (Å)	2.05	1.90	1.72
R_{sym}	8.5 (53.2)	5.4 (48.6)	7.2 (54.0)
$I/\sigma I$	24.8 (2.1)	42.9 (3.4)	34.2 (2.9)
Completeness (%)	97.8 (85.0)	98.7 (88.7)	98.8 (89.0)
Redundancy	12.5 (5.1)	12.8 (6.5)	13.9 (9.3)
Refinement			
Resolution (Å)		36.7–1.90	30.2–1.72
No. reflections		27,733	39,069
R_{work}/R_{free}		0.209/0.261	0.179/0.210
No. atoms			
Protein		2675	2741
Ligand/ion		16 (4 EDO)	40 (1 ATP, 2 Mg, 1 MLI)
Water		160	276
B-factors			
Protein		41.7	29.9
Ligand/ion		46.3	21.4
Water		49.3	39.2
Root mean square deviations			
Bond lengths (Å)		0.019	0.017
Bond angles (°)		1.585	1.707

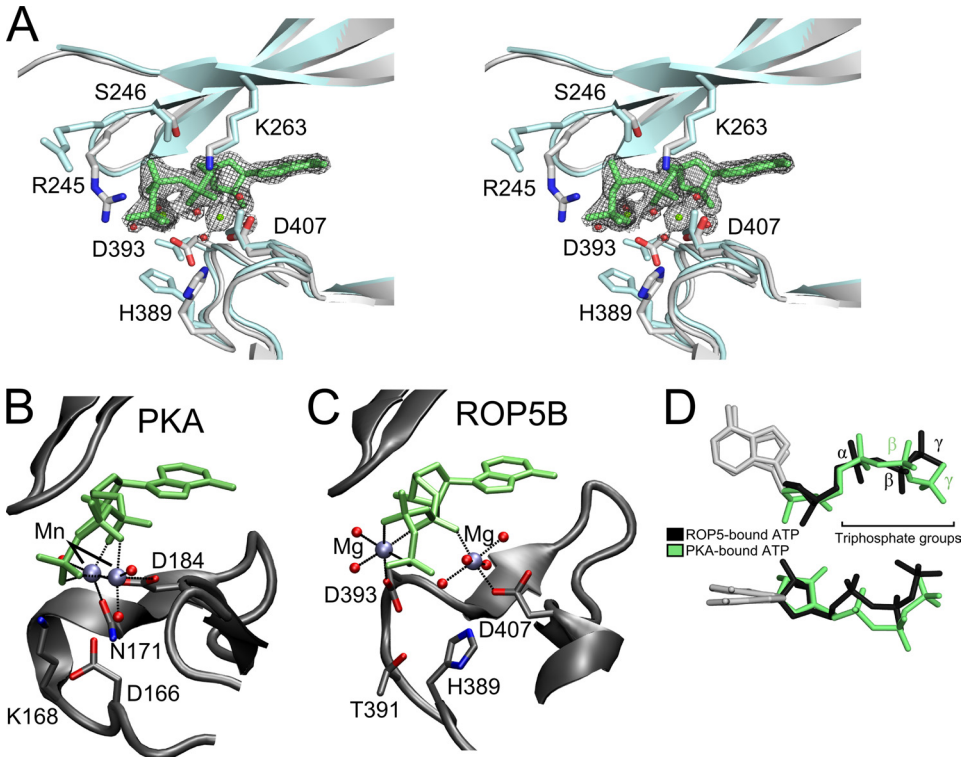

FIGURE 3. **ROP5 binds ATP in an unusual conformation.** *A*, a stereo view of the pseudoactive site of ROP5B$_I$ is shown comparing the ATP-bound (*gray*) and unbound (*blue*) structures. Residues that make contact with ATP are shown as *sticks*. The ATP and its associated Mg^{2+} and waters are superposed with the 1.72-Å $2F_o - F_c$ electron density map contoured at 2.5 σ. The PKA (*B*) and ROP5B$_I$ (*C*) active sites are shown with bound ATP in an orientation to highlight the magnesium conformation. *D,* the ATP molecules bound to ROP5 (*black*) or PKA (*green*) have been overlaid to highlight triphosphate conformation.

Toxoplasma ROP2 (34, 35), and mammalian ILK (16) and VRK3 (36) each appear to be locked in the closed conformation typical of active, ATP-bound kinases. This is in contrast to STRADα, which despite its degraded catalytic core, has maintained the Gly-rich P-loop, and appears to use the dynamics typically thought to be inherent in the kinase fold to allosterically regulate its binding partners (17, 37).

Surprisingly, given the conservation of the ATP-binding motifs, and despite being coordinated by two Mg^{2+} in the active site, the ROP5-bound ATP triphosphate is in a substantially different conformation than found in PKA and other active kinases (Fig. 3, *B–D*). The PKA conformation has been confirmed by simulation to be that competent for catalysis (33, 38). Simulation studies have also shown that the efficiency of phos-

phoryl transfer by a protein kinase is sensitive to motions on the order of 0.1 Å (39). As each of the phosphorous atoms of the ATP are displaced by ~2 Å in the ROP5 structure from their positions in that of PKA, we would predict these differences to have a significant deleterious effect on the phosphoryl transfer activity of ROP5. This is consistent with the lack of detectable catalytic activity of either the wild-type or H389D ROP5B$_I$.

These distortions in the ATP conformation bound in the ROP5 pseudoactive site are mediated by an unusual coordination of Mg^{2+} cations. Despite having conserved both the canonical M1 (the "DFG" motif, Asp-184 in PKA, Asp-407 in ROP5) and M2 (Asn-171 in PKA, Asn-394 in ROP5) Mg^{2+}-binding residues, the M2 site in ROP5 has been shifted. Although PKA Asp-184 contributes to the coordination of both Mg^{2+} ions, ROP5 Asp-407 coordinates only the M1 Mg^{2+}. Also, in ROP5 the Asn-394 side chain is orthogonal to the orientation found in PKA and, instead, Asp-393 of ROP5 is coordinating the M2 Mg^{2+}. ROP5 Asn-394, however, plays a supporting role, hydrogen bonding both with one of the waters that coordinates the M2 Mg^{2+} and with the His-389 backbone carbonyl, assisting in orienting it toward the ATP γ-phosphate (supplemental Fig. S5). Together, these differences result in a more splayed-out conformation of ATP than found in PKA (Fig. 3*D*). It is important to note that neither the displaced Mg^{2+} coordination nor the distorted ATP conformation would be predicted from either the primary sequence of ROP5 or its apo-structure.

In addition to these major differences in Mg^{2+} coordination, ROP5 makes several other unusual contacts with its bound ATP. In many kinases, a Lys two residues C-terminal to the catalytic Asp (Lys-168 in PKA) assists in orienting the triphosphate (Fig. 3*B*). In ROP5, this residue is Thr-391 that is hydrogen bonding with Asp-393 (supplemental Fig. S5*A*). In apparent compensation, ROP5 Arg-245 (a bulky hydrophobic in most kinases; Phe-54 in PKA) swings down from the P-loop above the ATP to salt bridge with the γ-phosphate (Fig. 3*A*). In addition, ROP5 Ser-246 (Gly-55 in PKA) hydrogen bonds with the ATP β-phosphate. This substitution in the P-loop, however, is unlikely to participate in distorting the ATP conformation, as other, active kinases have equivalent substitutions at this position. For example, casein kinase 2 from both mammals and plants has a Ser at the equivalent position to ROP5 Ser-246, which makes similar contacts with the nucleotide β-phosphate but does not perturb the nucleotide conformation (PDB code 1DAW, supplemental Fig. S6), nor does it affect catalytic activity.

Although ROP5 His-389 (the catalytic Asp-166 in PKA) is oriented toward the ATP γ-phosphate, it is relatively distant (4–5 Å) to form an effective salt bridge. However, in three of the allelic isoforms of ROP5, His-389 is replaced by an Arg (supplemental Fig. S1). Although we do not have structural information on these isoforms, modeling predicts that with its extended reach, such an Arg would directly coordinate the ATP γ-phosphate (supplemental Fig. S5*B*).

The ROP5 Pseudokinase Domain Exists in a Conformation That Likely Precludes Catalysis—Although the binding of ATP in a conformation suitable for catalysis is critical for phosphoryl transfer, the global conformation of the kinase fold plays an important role in stabilizing additional conserved intramolecular contacts that facilitate catalysis. Given the lack of conformational change between the ATP-bound and unbound structures of ROP5 (supplemental Fig. S4), it is difficult to assess whether the domain is in a truly "active" conformation. One of the hallmarks of the active conformation of a protein kinase is the clamping down of the P-loop onto the bound nucleotide. Regardless of nucleotide occupancy, the P-loop of ROP5 aligns more closely with that of active PKA (PDB code 1ATP; 3.1 Å root mean square deviation for 217 of 351 Cα atoms) as compared with an inactive conformation (PDB code 1SYK (40); 3.9 Å root mean square deviation for 224 of 351 Cα atoms; supplemental Fig. S7, *A* and *B*). On the other hand, in the ROP5 structures, helix C is in a substantially different conformation than in PKA (supplemental Fig. S7). The relative position of this helix can, however, vary greatly among the structures of different kinases, and even between structures of the same kinase (*e.g.* p38; PDB codes 1CM8 and 1YWR (41, 42)). The conserved Glu in the center of helix C makes a critical hydrogen bond with the catalytic Lys (30). In ROP5, Glu-281 may be the conserved glutamate in question. However, the ROP5 helix C is in an orientation that flips Glu-281 out and creates an empty cavity where the conserved Glu would normally sit during the catalytic cycle. Interestingly, in the ATP-bound structure of ROP5, this space is filled by a crystallographic malonate, whose carboxylate interacts with Lys-263 in a manner analogous to the helix C Glu (supplemental Fig. S7, *C* and *D*). It is also important to note that this cavity near ROP5 helix C creates a gap in the "regulatory spine," a conserved series of contacts that appear to be required for a catalysis in an active enzyme (43). Although the present structures do not suggest it, we cannot exclude the possibility that, under other conditions, the ROP5 helix C reorients to adopt a conformation more similar to that observed in other, active kinases.

Structurally Conserved Regulatory Elements Bridge Polymorphic Surfaces on ROP5—Many protein kinases are activated by the structural transition of their activation segments from disordered to ordered. The activation segments comprise the sequence from the conserved DFG to APE motifs (44) (Asp-407 to Glu-431 in ROP5). This transition can be caused both by interaction with regulatory molecules and by phosphorylation of residues in the activation loop. The activation segment of ROP5, however, appears locked in an ordered conformation, as it is well ordered in each of our structures, independent of the ATP-binding state (supplemental Figs. S4 and S8). In ROP5, the DFG Gly has been substituted for Ser (Ser-409) and two prolines align with both the activation loop phosphorylation site and GT motif Thr of PKA (supplemental Fig. S8), which may help rigidify the ROP5 loop.

The ROP5 pseudokinase domain, like other members of the rhoptry kinase family has an N-terminal extension (NTE) in primary sequence that plays a major role in allowing profiling methods to distinguish the members of this family from other kinases (7). In the structures of two of closest relatives of ROP5, the non-ATP-binding pseudokinases ROP2 and ROP8, the center of the NTE has an extended conformation, with a loop whose side chains tuck between the N- and C-lobes and occlude the ATP-binding site (34, 35) (supplemental Fig. S9). In ROP5,

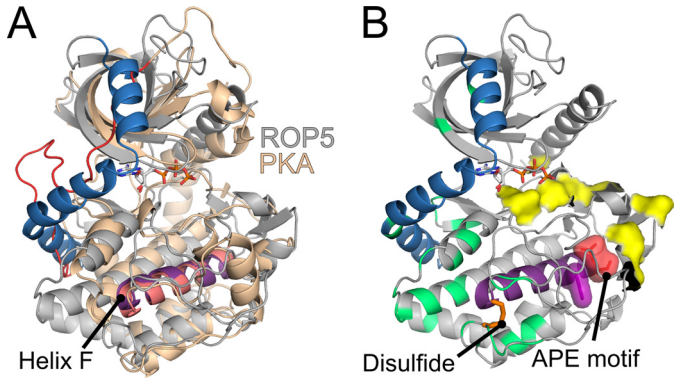

FIGURE 4. **Structurally conserved regulatory elements in ROP5 bridge polymorphic surfaces.** *A,* the structures of ROP5B$_I$ (*gray* with NTE in *blue*) are overlaid PKA (PDB code 1ATP; *tan* with C-terminal linker in *red*). The hydrophobic α-helix F is highlighted *purple* for ROP5 and *pink* for PKA. The ROP5 ATP is shown as *sticks*. *B,* the ATP-bound ROP5B$_I$ structure colored as in *A*, and polymorphic residues are indicated in *green* (surface exposed) or as a *yellow* surface (near active site). A disulfide bond at the C terminus of helix F, conserved throughout the rhoptry kinase family, is shown as *orange sticks*. The ROP5 APE motif is indicated as *red space filling*, and the conserved Trp-447 of helix F against which the APE motif packs is indicated in *purple space filling*.

however, the NTE forms three α-helices that wrap around the structure, tethering the N- and C-lobes (Fig. 4*A* and supplemental Fig. S9). Although these helices pack tightly against the N-lobe, none of the residues occlude the ATP-binding site. Interestingly, the C-terminal linker of the AGC family (which includes PKA and PKC) occupies the same three-dimensional space as the NTE, but arises from the opposite side of the primary sequence (Fig. 4 and supplemental Fig. S3). The C-terminal region of the AGC family terminates in a hydrophobic motif, whose two Phe are buried in the kinase N-lobe. Analogously, the ROP5 NTE terminates in the conserved Trp-215, which is also buried in the N-lobe (supplemental Fig. S9B). In the AGC family, divergence of this C-terminal span has been suggested as a major mechanism of diversification of regulatory elements in the family (13). Strengthening the analogy, the sequences of the rhoptry kinase NTE are quite divergent, even among close relatives (supplemental Fig. S9*C*). The space occupied by the ROP5 NTE has been suggested to be a critical hinge region that can alter the interdomain motions of the N- and C-lobes of a kinase (13). Thus the varied rhoptry kinase NTE and AGC C-terminal sequences may represent convergent solutions to the problem of regulation.

A recently proposed model suggests the various regulatory elements of protein kinases are structurally anchored on the conserved hydrophobic α-helix F (43), which serves as a central point of allosteric cross-talk between the regulatory elements. In ROP5, as with other kinases, the center of helix F packs against the activation segment (Fig. 4). Interestingly, the activation segment of ROP5 has several substitutions that are typical of differences between isoforms (rather than strains; Fig. 4*B* and supplemental Fig. S1). The C terminus of the ROP5 helix F has a disulfide bridge (Cys-458 to Cys-492), conserved in many rhoptry kinases (45), that directly anchors it to the polymorphic patch from which the NTE extends (Fig. 4*B*). The high selective pressure on this surface strongly implicates it as a binding site for the proteins with which ROP5 may interact to affect virulence. As our *in vivo* mutagenesis data demonstrate the ROP5 pseudoactive site is required for its full function (Fig. 1*D*), it is tempting to hypothesize that the NTE and hydrophobic helix F serve to allosterically link the ROP5 pseudoactive site to the two polymorphic regions on its surface, which may represent sites at which ROP5 interacts with its downstream targets. Such a model is consistent with recent structural studies that demonstrate that STRADα (17) and ILK (16) regulate their binding partners through interaction with their activation segments and pseudoactive sites.

DISCUSSION

We have solved the structure of the pseudokinase domain of ROP5, a protein that is critical for the ability of *Toxoplasma* to cause disease and is the major determinant of strain-specific variation in virulence (10, 11). The rhoptry kinase family is specific to coccidian parasites, and is highly enriched in proteins that are predicted to be secreted (7), implicating the family as a focal point in the interaction between *Toxoplasma* and its varied hosts. Recent work demonstrated that the ROP5 pseudokinase domain contains many polymorphic residues that appear to be under strong positive selection (10). Building on this, we have shown that these polymorphic residues throughout the primary sequence are concentrated within a major surface. Our results indicate a strong selective pressure has operated on this region of the protein, which is adjacent to the hinge between the N- and C-lobes of the kinase fold. Taken together, these data suggest that ROP5 mediates its effect on virulence through interaction with and dysregulation of its target or targets using this surface. Although we cannot yet know whether the binding partners are of host or parasite origin, the fact that the ROP5 proteins reside on the parasitophorous vacuolar membrane and are exposed to the host cytosol (45–47), suggests that the potential binding partner(s) derive from the host.

The structure of ROP5 is especially interesting in its relationship with current thinking of both kinase and pseudokinase function. Analysis of proteins with kinase folds often invokes the conservation of canonical motifs (30), whose contribution to catalysis has been exhaustively studied structurally, biochemically, and through simulation. Of the pseudokinases whose structures are known, ROP5 has among the greatest conservation of the canonical kinase motifs, apparently lacking only the catalytic Asp, suggesting that ROP5 should be competent to bind ATP in a canonical conformation competent for catalysis. Remarkably, in the structure of ROP5B$_I$ bound to ATP, the canonical ATP-binding residues in the ROP5 pseudoactive site have evolved to stabilize a surprisingly non-canonical conformation of ATP, which appears protected from hydrolysis. As shown here, this ATP conformation appears incompatible with catalytic activity, even with the re-introduction of the catalytic Asp by mutagenesis. Thus, it is possible that even proteins with apparently complete canonical kinase motifs may not be catalytically active, which provides an interesting corollary to the recent discovery that several proteins originally thought to be pseudokinases appear to have maintained their catalytic activities even with a non-canonical active site (19, 20). For instance, Wnk1 originally appeared to lack a catalytically active Lys, but instead has adapted to use a non-canonical Lys from a different position in its primary sequence (18). CASK, on the

other hand, whereas missing the Mg^{2+}-coordinating DFG motif, has adapted a new set of residues to form a magnesium-independent active site (19). Interestingly, in CASK, mutagenesis of the canonical catalytic Asp and Lys did not alter its catalytic activity (19), indicating that its atypical active site truly acts independently from many of the canonical motifs. This is in contrast to our mutagenesis data of ROP5, in which substitution to restore the canonical HRD motif Asp resulted in a less functional (but, biologically, not inactive) protein *in vivo*. Particular care should be taken when ascribing function or nonfunction to novel sequences; nevertheless, and although we cannot prove unequivocally that the ROP5 proteins described here lack catalytic activity, the presence of a basic residue in place of the catalytic Asp, the altered conformation of the bound ATP, and our failure to detect any activity in biochemical assays, even using a mutant form engineered to reintroduce the Asp, makes the possibility of ROP5 being a functional kinase extremely unlikely.

By examining the kinomes of both humans and *Toxoplasma*, we have identified a potential subclass of pseudokinases based on their convergent evolution of the substitution of the canonical HRD motif with an HGB motif. We confirmed the importance of this motif by testing the *in vivo* activity of ROP5 in which a charge-swap mutation had replaced its basic Arg to restore the canonical Asp. *In vitro*, such protein maintained its ability to bind ATP, although it was still not catalytically active. *In vivo*, R389D mutant ROP5 was able to partially complement the virulence of a Δ*rop5* phenotype, but to a significantly lesser extent as compared with complementation with the wild-type ROP5. This is consistent with the proposed role of ROP5 as a molecular scaffold rather than as an atypical, active enzyme. By extension, our data implicate the conserved non-canonical HGB motif as important to the function of multiple other pseudokinases in a variety of organisms. Hence, pseudokinases may not be the outliers as they first appeared; just as diligent research has elucidated general principles that govern a catalytic activity of the kinase, with further study the principles that govern the functioning of specific families of pseudokinases should soon be determinable.

Acknowledgments—We thank Arvin Dar for suggesting the ATP-Sepharose pull-down experiment, Mark Wilson and Tim Fenn for crystallographic software assistance, the Brünger lab for crystallization space, members of the Boothroyd lab for thoughtful suggestions, and Eva LaDow, Kara Norman, Selena Sagan, Mark Wilson, and Rich Yu for critical comments on the manuscript.

REFERENCES

1. Kuriyan, J., and Cowburn, D. (1997) *Annu. Rev. Biophys. Biomol. Struct.* **26,** 259–288
2. Pawson, T. (2007) *Curr. Opin. Cell Biol.* **19,** 112–116
3. Boudeau, J., Miranda-Saavedra, D., Barton, G. J., and Alessi, D. R. (2006) *Trends Cell. Biol.* **16,** 443–452
4. Boothroyd, J. C., and Dubremetz, J. F. (2008) *Nat. Rev. Microbiol.* **6,** 79–88
5. Bradley, P. J., and Sibley, L. D. (2007) *Curr. Opin. Microbiol.* **10,** 582–587
6. Saeij, J. P., Coller, S., Boyle, J. P., Jerome, M. E., White, M. W., and Boothroyd, J. C. (2007) *Nature* **445,** 324–327
7. Peixoto, L., Chen, F., Harb, O. S., Davis, P. H., Beiting, D. P., Brownback, C. S., Ouloguem, D., and Roos, D. S. (2010) *Cell Host Microbe* **8,** 208–218
8. Saeij, J. P., Boyle, J. P., Coller, S., Taylor, S., Sibley, L. D., Brooke-Powell, E. T., Ajioka, J. W., and Boothroyd, J. C. (2006) *Science* **314,** 1780–1783
9. Taylor, S., Barragan, A., Su, C., Fux, B., Fentress, S. J., Tang, K., Beatty, W. L., Hajj, H. E., Jerome, M., Behnke, M. S., White, M., Wootton, J. C., and Sibley, L. D. (2006) *Science* **314,** 1776–1780
10. Reese, M. L., Zeiner, G. M., Saeij, J. P., Boothroyd, J. C., and Boyle, J. P. (2011) *Proc. Natl. Acad. Sci. U.S.A.* **108,** 9625–9630
11. Behnke, M. S., Khan, A., Wootton, J. C., Dubey, J. P., Tang, K., and Sibley, L. D. (2011) *Proc. Natl. Acad. Sci. U.S.A.* **108,** 9631–9636
12. Knight, Z. A., and Shokat, K. M. (2005) *Chem. Biol.* **12,** 621–637
13. Kannan, N., Haste, N., Taylor, S. S., and Neuwald, A. F. (2007) *Proc. Natl. Acad. Sci. U.S.A.* **104,** 1272–1277
14. Pellicena, P., and Kuriyan, J. (2006) *Curr. Opin. Struct. Biol.* **16,** 702–709
15. Jura, N., Shan, Y., Cao, X., Shaw, D. E., and Kuriyan, J. (2009) *Proc. Natl. Acad. Sci. U.S.A.* **106,** 21608–21613
16. Fukuda, K., Gupta, S., Chen, K., Wu, C., and Qin, J. (2009) *Mol. Cell* **36,** 819–830
17. Zeqiraj, E., Filippi, B. M., Deak, M., Alessi, D. R., and van Aalten, D. M. (2009) *Science* **326,** 1707–1711
18. Min, X., Lee, B. H., Cobb, M. H., and Goldsmith, E. J. (2004) *Structure* **12,** 1303–1311
19. Mukherjee, K., Sharma, M., Urlaub, H., Bourenkov, G. P., Jahn, R., Südhof, T. C., and Wahl, M. C. (2008) *Cell* **133,** 328–339
20. Shi, F., Telesco, S. E., Liu, Y., Radhakrishnan, R., and Lemmon, M. A. (2010) *Proc. Natl. Acad. Sci. U.S.A.* **107,** 7692–7697
21. Donald, R. G., and Roos, D. S. (1995) *Proc. Natl. Acad. Sci. U.S.A.* **92,** 5749–5753
22. Ong, Y. C., Reese, M. L., and Boothroyd, J. C. (2010) *J. Biol. Chem.* **285,** 28731–28740
23. Otwinowski, Z., and Minor, W. (1997) in *Methods in Enzymology: Macromolecular Crystallography, Part A* (Carter, C. W., Jr., and Sweet, R. M., eds) Vol. 276, pp. 307–326, Academic Press, New York
24. Terwilliger, T. (2004) *J. Synchrotron Radiat.* **11,** 49–52
25. Terwilliger, T. C., and Berendzen, J. (1999) *Acta Crystallogr. D Biol. Crystallogr.* **55,** 849–861
26. Adams, P. D., Afonine, P. V., Bunkóczi, G., Chen, V. B., Davis, I. W., Echols, N., Headd, J. J., Hung, L. W., Kapral, G. J., Grosse-Kunstleve, R. W., McCoy, A. J., Moriarty, N. W., Oeffner, R., Read, R. J., Richardson, D. C., Richardson, J. S., Terwilliger, T. C., and Zwart, P. H. (2010) *Acta Crystallogr. D Biol. Crystallogr.* **66,** 213–221
27. Emsley, P., Lohkamp, B., Scott, W. G., and Cowtan, K. (2010) *Acta Crystallogr. D Biol. Crystallogr.* **66,** 486–501
28. McCoy, A. J., Grosse-Kunstleve, R. W., Adams, P. D., Winn, M. D., Storoni, L. C., and Read, R. J. (2007) *J. Appl. Crystallogr.* **40,** 658–674
29. Chen, V. B., Arendall, W. B., 3rd, Headd, J. J., Keedy, D. A., Immormino, R. M., Kapral, G. J., Murray, L. W., Richardson, J. S., and Richardson, D. C. (2010) *Acta Crystallogr. D Biol. Crystallogr.* **66,** 12–21
30. Hanks, S. K., and Hunter, T. (1995) *FASEB J.* **9,** 576–596
31. Cameron, A. J., Escribano, C., Saurin, A. T., Kostelecky, B., and Parker, P. J. (2009) *Nat. Struct. Mol. Biol.* **16,** 624–630
32. Valiev, M., Kawai, R., Adams, J. A., and Weare, J. H. (2003) *J. Am. Chem. Soc.* **125,** 9926–9927
33. Turjanski, A. G., Hummer, G., and Gutkind, J. S. (2009) *J. Am. Chem. Soc.* **131,** 6141–6148
34. Qiu, W., Wernimont, A., Tang, K., Taylor, S., Lunin, V., Schapira, M., Fentress, S., Hui, R., and Sibley, L. D. (2009) *EMBO J.* **28,** 969–979
35. Labesse, G., Gelin, M., Bessin, Y., Lebrun, M., Papoin, J., Cerdan, R., Arold, S. T., and Dubremetz, J. F. (2009) *Structure* **17,** 139–146
36. Scheeff, E. D., Eswaran, J., Bunkoczi, G., Knapp, S., and Manning, G. (2009) *Structure* **17,** 128–138
37. Zeqiraj, E., Filippi, B. M., Goldie, S., Navratilova, I., Boudeau, J., Deak, M., Alessi, D. R., and van Aalten, D. M. (2009) *PLoS Biol.* **7,** e1000126
38. Khavrutskii, I. V., Grant, B., Taylor, S. S., and McCammon, J. A. (2009) *Biochemistry* **48,** 11532–11545
39. Henkelman, G., LaBute, M. X., Tung, C. S., Fenimore, P. W., and McMahon, B. H. (2005) *Proc. Natl. Acad. Sci. U.S.A.* **102,** 15347–15351

40. Wu, J., Yang, J., Kannan, N., Madhusudan, Xuong, N. H., Ten Eyck, L. F., and Taylor, S. S. (2005) *Protein Sci.* **14,** 2871–2879
41. Bellon, S., Fitzgibbon, M. J., Fox, T., Hsiao, H. M., and Wilson, K. P. (1999) *Structure* **7,** 1057–1065
42. Golebiowski, A., Townes, J. A., Laufersweiler, M. J., Brugel, T. A., Clark, M. P., Clark, C. M., Djung, J. F., Laughlin, S. K., Sabat, M. P., Bookland, R. G., VanRens, J. C., De, B., Hsieh, L. C., Janusz, M. J., Walter, R. L., Webster, M. E., and Mekel, M. J. (2005) *Bioorg. Med. Chem. Lett.* **15,** 2285–2289
43. Kornev, A. P., Taylor, S. S., and Ten Eyck, L. F. (2008) *Proc. Natl. Acad. Sci. U.S.A.* **105,** 14377–14382
44. Nolen, B., Taylor, S., and Ghosh, G. (2004) *Mol. Cell* **15,** 661–675
45. El Hajj, H., Demey, E., Poncet, J., Lebrun, M., Wu, B., Galéotti, N., Fourmaux, M. N., Mercereau-Puijalon, O., Vial, H., Labesse, G., and Dubremetz, J. F. (2006) *Proteomics* **6,** 5773–5784
46. Reese, M. L., and Boothroyd, J. C. (2009) *Traffic* **10,** 1458–1470
47. El Hajj, H., Lebrun, M., Fourmaux, M. N., Vial, H., and Dubremetz, J. F. (2007) *Cell. Microbiol.* **9,** 54–64
48. Manning, G., Whyte, D. B., Martinez, R., Hunter, T., and Sudarsanam, S. (2002) *Science* **298,** 1912–1934